Inorg. Chem. **2006**, *45*, 2104–2111

Substitution of Au or Hg into $BaTl_2$ and $BaIn_2$. New Ternary Examples of Smaller $CeCu_2$-Type Intermetallic Phases

Jing-Cao Dai and John D. Corbett*

Ames Laboratory-DOE[1] and Department of Chemistry, Iowa State University, Ames, Iowa 50010

Received November 1, 2005

The compounds $BaAu_{0.40(2)}Tl_{1.60(7)}$ (**1**), $BaAu_{0.36(4)}In_{1.64(4)}$ (**2**), and $BaHg_{0.92(2)}In_{1.08(2)}$ (**3**) have been prepared by high-temperature techniques. Single-crystal X-ray diffraction shows that these have the orthorhombic $CeCu_2$-type structure, *Imma*, $Z = 4$ (a = 5.140(1), 5.104(1), 5.145(1) Å; b = 8.317(2), 8.461(2), 8.373(2) Å; c = 8.809(2), 8.580(2), 8.715(2) Å, respectively). The structure consists of a four-linked honeycomblike polyanion (4^26^38) of $^3_\infty[Tr_2]^{2-}$ (Tr = In or Tl) with encapsulated Ba^{2+} cations. The Au or Hg randomly replace Tr in a single type of site. The two gold phases exhibit appreciable nonstoichiometry ranges. Band calculations (EHTB) demonstrate that the three compounds are electron-poor and metallic, and the latter has been confirmed for **1** through resistivity and magnetic susceptibility measurements. The orthorhombic structure of **1** contrasts with the hexagonal structure of $BaTl_2$ ($CaIn_2$-type, $P6_3/mmc$), a change that appears to be driven by substitution of the smaller Au atoms into the polyanion network. Relativistic effects for the heavier Au and Hg are evidently responsible for decreases in lattice parameters and bond lengths from $BaIn_2$ to those in isostructural **2** and **3**.

Introduction

Polar intermetallic phases generated by reduction of triel elements (Tr = Al−Tl) by electropositive alkali or alkaline-earth metals are attracting increased interest owing to not only their fascinating structures but also their peculiar chemistry in the nonclassical valence region.[2] Unlike alkali metal−triel compounds, which frequently present a rich collection of discrete cluster anions, as in K_8In_{11},[3] $K_8In_{10}Zn$,[4] $Na_3K_8Tl_{13}$,[5] and $K_{34}Li_{12.7}In_{92.3}$,[6] the alkaline-earth metals with the same triels form more complex three-dimensional anionic networks in which the smaller number of cations are encapsulated. Some very interesting examples have been reported, such as binary $SrIn_4$,[7] Sr_3In_5,[8] and ternary $CaTnIn_2$ (Tn = Pd, Pt, Au),[9] Ca_2CuIn_3,[10] Ba_2AuTl_7,[11] $BaAuTl_3$,[12] and $SrTnTl_2$ (Tn = Pd, Pt).[13] In such 3D frameworks, the combined problems of lattice stability, size match, and optimal bonding interactions for cations within the anionic network are more complex than in most systems with discrete clusters. However, the same systems seem particularly suitable as far as understanding significant chemical questions, i.e., phase stability, structural derivations and transformations that derive from dimensional matrix effects, and chemical bonding. So far, the chemistry of these systems has remained largely unexplored. Here we report on three new compounds in the ternary Ba−(Au,Hg)−(In,Tl) systems that are isostructural with orthorhombic $CeCu_2$, a lower-symmetry relative of the $CaIn_2$ type

Experimental Section

Powder X-ray Diffraction and EDX Analyses. Powder diffraction investigations were carried out on samples mounted inside the glovebox between two pieces of Mylar with the help of a little Apiezon grease. The data were recorded at ~22 °C on a Huber

* To whom correspondence should be addressed. Email: jdc@ameslab.gov.

(1) This research was supported by the Office of the Basic Energy Sciences, Materials Sciences Division, U. S. Department of Energy (DOE). The Ames Laboratory is operated for the DOE by Iowa State University under Contract No. W-7405-Eng-82.

(2) (a) Nesper, R. *Angew. Chem., Int. Ed. Engl.* **1991**, *30*, 789. (b) Belin, C. H. E.; Tillard-Charbonnel, M. *Prog. Solid State Chem.* **1993**, *22*, 5. (c) Corbett, J. D. In *Chemistry, Structure and Bonding of Zintl Phases and Ions*; Kauzlarich, S. M., Ed.; VCH Publishers: New York, 1996; Chapter 4. (d) Corbett, J. D. *Angew. Chem., Int. Ed.* **2000**, *39*, 670.
(3) Sevov, S. C.; Corbett, J. D. *Inorg. Chem.* **1991**, *30*, 4875.
(4) Sevov, S. C.; Corbett, J. D. *Inorg. Chem.* **1993**, *32*, 1059.
(5) Dong, Z.-C.; Corbett, J. D. *J. Am. Chem. Soc.* **1995**, *117*, 6447.
(6) Li, B.; Corbett, J. D. *J. Am. Chem. Soc.* **2005**, *127*, 926.
(7) Seo, D.-K.; Corbett, J. D. *J. Am. Chem. Soc.* **2000**, *122*, 9621.
(8) Seo, D.-K.; Corbett, J. D. *J. Am. Chem. Soc.* **2002**, *124*, 415.
(9) Hoffmann, R.-D.; Pöttgen, R.; Landrum, G. A.; Dronskowski, R.; Künen, B.; Kotzyba, G. Z. *Anorg. Allg. Chem.* **1999**, *625*, 789.
(10) Sysa, L. V.; Kalychak, Ya. M. *Crystallogr. Rep.* **1993**, *38*, 278.
(11) Liu, S.; Corbett, J. D. *Inorg. Chem.* **2004**, *43*, 2471.
(12) Liu, S.; Corbett, J. D. *Inorg. Chem.* **2004**, *43*, 4988.
(13) Liu, S.; Corbett, J. D. *Inorg. Chem.* **2003**, *42*, 4898.

10.1021/ic051891k CCC: $33.50
Published on Web 02/10/2006

670 Guinier camera equipped with an area sensitive detector and Cu Kα radiation ($\lambda = 1.540598$ Å). The step size was set at 0.005°, and the exposure time was 30 min. Least-squares refinements to obtain unit cell parameters were done with the aid of the Rietica program.[14]

To confirm the Au/Tl ratio in **1**, a freshly crushed sample of single crystals was mounted in a Hexland transfer device in a N_2-filled glovebox and then inserted into a JEOL 840A SEM equipped with an IXRF X-ray analyzer system and a Kevex Quantum light-element detector for multiple EDX data collections.

Syntheses. The compounds were prepared from high-purity elements by high-temperature solid-state synthesis techniques described previously.[7,8,11−13] The reagents were dendritic Ba (99.9%, Alfa-Aesar), Au sheet (99.997%, Ames Lab), Hg (instrument grade, Fisher), In tear drops (99.99%, Alfa-Aesar), and Tl granules (99.999%, Alfa-Aesar), which were handled in a N_2-filled glovebox in which the moisture levels were controlled below 0.1 ppm (volume). The surfaces of Tl and In were scraped clean with a scalpel before use, whereas the Ba sample remained shiny. The desired proportion of the weighed elements was first welded into metal (Ta, Nb) tubing, which was then jacketed in evacuated fused silica containers and subsequently heated in resistance furnaces.

In a search for new ternary Ba−Au−Tl intermetallics related to hexagonal $BaTl_2$ or $BaAu_2$,[15] single crystals that refined as $BaAu_{0.4}Tl_{1.6}$ (**1**) were obtained from a reaction with a Ba/Au/Tl proportion of 1:0.4:1.6 in Nb tubing at 1000 °C that was then quenched in water and subsequently annealed at 600 °C for 4 days. This reaction resulted in a single-phase sample (>95%) of **1**, as judged by comparison of its Guinier powder pattern with that later calculated for the refined structure. The proportions in **1** were found to be $BaAu_{0.40(2)}Tl_{1.60(7)}$ by multiple EDX analyses on a single crystal, consistent with the loaded composition within the error limits. Moreover, high-quality samples (>90%) of a series of isotypic $BaAu_xTl_{1-x}$ products were similarly obtained over a range of $x = 0.1$ to at least 0.5 Au (see Supporting Information, Figure S1).

Single crystals of isotypic $BaAu_{0.36(4)}In_{1.64(4)}$ (**2**) were first obtained in about 70% yield, plus ∼30% unknowns, from a $BaAu_{0.5}In_{1.5}$ composition under the same reaction conditions but in tantalum tubing. Comparable but apparent single phase samples of a series of isotypic $BaAu_xIn_{2-x}$ ($0 \le x \le \sim 0.4$) compositions with only small variations of the lattice constants were subsequently obtained from In-richer compositions under the same conditions (Supporting Information, Table S17, Figure S2). No Ba_3Au_2 was seen in either study.

The isotypic $BaHg_{0.92(2)}In_{1.08(2)}$ (**3**) was first discovered as an unexpected result from an attempt to synthesize ternary Ba−Hg−In phases isostructural with either monoclinic (*C*2/*m*) $BaHg_xTl_{4-x}$[16] ($0 \le x \le 1$, $SrIn_4$-type[7]) or tetragonal ($P4_2/mnm$) $BaHg_2Tl_2$[16] (reportedly $BiPb_3Pt$-type[15]). Product **3** was obtained in more than 90% yield from a 1:1:1 mixture Ba/Hg/In in a Ta tube that was heated at 730 °C for 1 day, quenched in water, annealed at 400 °C for 1 week, then cooled to 160 °C at 0.5 °C/h, and finally cooled at 3 °C/h to room temperature. (The observed and calculated Guinier patterns are shown in Supporting Information, Figure S3). Single crystals of all three new phases are silvery, brittle, and very sensitive to air.

Structure Determinations. Blocklike single crystals of **1**, **2**, and **3** were mounted in glass capillaries inside a N_2-filled glovebox designed for crystal mounting and then separately transferred to Bruker Smart APEX CCD diffractometer for data collection at 293(2) K with Mo Kα radiation ($\lambda = 0.71073$ Å). A total of 1315 frames was collected from each with an exposure time of 10 s per frame. No evidence for any superstructure, ordered or not, was encountered. The reflection intensities were integrated with the SAINT subprogram in the SMART software package[17] for the orthorhombic cell initially indicated from indexing 363 reflections for **1** and 477 reflections for **2** and **3**. Empirical absorption corrections were made with the SADABS program.[18] Space group determination by the XPREP program in the SHELXTL 6.1 software package[19] suggested *Ima*2 (No. 46, CFOM = 11.2) or *Imma* (No. 74, CFOM = 12.7) on the basis of systematic absences, but the intensity statistics did not give very clear indications of an acentric or centric space group ($|E^2 - 1| = 0.839$ for **1**, 0.872 for **2**, and 0.815 for **3**). At the beginning, the structure of **1** was solved in the acentric *Ima*2 space group after the centric *Imma* would not yield a structural solution by direct methods, but the possibility of *Imma* still could not be eliminated because of some large correlation matrix elements. Finally, the structure of **1** was successfully solved in correct centric space group *Imma* by Patterson methods, and the structures of **2** and **3** were also successfully solved by the same approach. A similar result was also obtained for isostructural $SrAg_{0.8(2)}In_{1.2(2)}$ which had only been refined in space group *Ima*2 (Supporting Information).[20]

In these structures, a single 4*e* site is occupied by Ba, and an 8*h* site contains a disordered mixture of the later metals. The mixed sites refined as written for **2** and **3**. Inasmuch as Tl and Au in **1** cannot be well distinguished by X-ray diffraction, the Tl/Au ratio was set at 20:80 according to the initial loading, the formation of a single high-purity phase therefrom, and the EDX analysis results (above). Final refinements with anisotropic displacement parameters converged at R1 = 0.0367 for **1**, 0.0394 for **2** and 0.0258 for **3**. The largest residual peak and hole in the ΔF maps were, for **1**, 4.37 and −5.57 e·Å^{-3} at 0.73 and 0.69 Å from the (Tl + Au) site, for **2**, 3.54 and −5.64 e·Å^{-3} at 0.69 and 0.70 Å from the (In + Au) site, and for **3**, 2.68 and −1.65 e·Å^{-3} at 0.86 and 0.69 Å from the Ba and the (In + Hg) sites, respectively.

Some crystallographic data are summarized in Table 1, and the atomic positions, as well as occupancy data and important bond lengths for all three compounds, are listed in Tables 2 and 3, respectively. More detailed crystallographic information as well as refinement data and anisotropic displacement parameters are in Supporting Information.

Property Measurements. Electrical resistivities of **1** were determined at 34 MHz over the range of 50−280 K by the electrodeless "Q" method with the aid of Hewlett-Packard 4342 A Q meter.[21] This used a 90.2 mg sample with grain diameters between 150 and 250 μm that had been dispersed with chromatographic alumina inside the glovebox and sealed in a Pyrex tube. The magnetic susceptibilities of **1** were measured for a 141.1 mg polycrystalline sample held between faces of two fused silica rods, as described previously.[3] Data were collected between 6 and 350 K with the aid of a Quantum Design (MPMS) SQUID magnetometer.

(14) Hunter, B. A. *LHPM-Rietica Rietveld*, Version 1.71; Australian Nuclear Science and Technology Organization: Menai, N. S. W., Australia, 1997.
(15) Villars, P.; Calvert, L. D. *Pearson*'s *Handbook of Crystallographic Data for Intermetallic Phases*, 2nd ed.; American Society for Metals: Metals Park, OH 1991.
(16) Dai, J.-C.; Corbett, J. D. unpublished results.
(17) *SMART*; Bruker AXS, Inc.; Madison, WI, 1996.
(18) Blessing, R. H. *Acta Crystallogr.* **1995**, *A51*, 33.
(19) *SHELXTL*; Bruker AXS, Inc.; Madison, WI, 2000.
(20) Liu, S.; Corbett, J. D. unpublished results.
(21) Zhao, J.-T.; Corbett, J. D. *Inorg. Chem.* **1995**, *34*, 378.

Table 1. Some Crystal and Structure Refinement Parameters for **1**, **2**, and **3**

compounds	**1**	**2**	**3**
empirical formula	$BaAu_{0.40(2)}Tl_{1.60(7)}$	$BaAu_{0.36(4)}In_{1.64(4)}$	$BaHg_{0.92(2)}In_{1.08(2)}$
fw	543.1	396.6	445.7
space group, *Z*	*Imma* (No. 74), 4	*Imma* (No. 74), 4	*Imma* (No. 74), 4
unit cell dimensions			
a (Å)	5.140(1)	5.104(1)	5.145(1)
b (Å)	8.317(2)	8.461(2)	8.373(2)
c (Å)	8.809(2)	8.580(2)	8.715(2)
V (Å^3)	376.6(1)	370.5(1)	375.4(1)
d_{calcd} (Mg/m^3)	9.580	7.098	7.885
μ (Mo Kα) (mm^{-1})	93.909	34.321	54.117
final *R* indices[b]			
R1, wR2 [$I > 2\sigma(I)$]	0.0367, 0.0992	0.0394, 0.0980	0.0258, 0.1094

[a] CCD diffractometer data. [b] $R1 = \sum(||F_o| - |F_c||)/\sum|F_o|$; $wR2 = \{\sum w[(F_o^2-F_c^2)^2]/\sum w[(F_o^2)^2]\}^{1/2}$.

Table 2. Atomic Positions and Isotropic Displacement Parameters (Å^2) for **1**, **2**, and **3**

atom	wyck	*x*	*y*	*z*	*U* (eq)	occup.
				1		
Ba	4*e*	0	1/4	0.9604(2)	0.017(1)	
Au/Tl	8*h*	0	0.5514(1)	0.6645(1)	0.015(1)	0.20(1)/0.80(4)[a]
				2		
Ba	4*e*	0	1/4	0.9515(2)	0.020(1)	
Au/In	8*h*	0	0.5582(2)	0.6635(1)	0.024(1)	0.18(2)/0.82[b]
				3		
Ba	4*e*	0	1/4	0.9583(1)	0.015(1)	
Hg/In	8*h*	0	0.5533(1)	0.6649(1)	0.018(1)	0.46(1)/0.54[b]

[a] EDX result. [b] Refined from X-ray data.

The measured resistivities of **1** yielded a ~42.9 $\mu\Omega$·cm value at room temperature with a mean temperature dependence of 0.18% K^{-1} (Figure S4, Supporting Information). The magnetic susceptibilities of **1** (Figure S5, Supporting Information) are small, positive, and almost temperature-independent, with $\chi_M \approx 8.4 \times 10^{-5}$ emu·mol^{-1} over 50−350 K after container and ion core corrections,[22] typical of a Pauli paramagnetic characteristic.

Band Calculations. Band structure calculations were made by the extended Hückel tight binding (EHTB) method with the aid of the CAESAR software.[23] The parameters (valence energies (eV), orbital exponents) used were as follows. Ba: 6s −4.760, 1.263; 6p −2.640, 1.263;[24] Tl: 6s −11.6, 2.52; 6p −5.8, 1.77;[25] In: 5s −12.6, 1.903; 5p −6.19, 1.677;[26] Au: 6s −10.92, 2.602; 6p −5.55, 2.584; 5d −15.076, 6.163, 0.6851, 2.794, 0.5696;[27] Hg: 6s −13.68, 2.649; 6p −8.47, 2.631; 5d −17.50, 6.436, 0.6438, 3.032, 0.5215.[28] For the situations with mixed metals on a single site, the symmetry was in each case lowered to *P*1, and two or four nonadjacent positions in the former 8*h* set were substituted by Au or Hg, respectively. Alternate choices of the heavy atom distributions did not make any appreciable difference as long as they were not interbonded. The relative weights of bonds **I**, **II**, and **III** in this method, including those intrinsic to the type (see Results and Discussion), turn out to be 4/4:1:2/2 heteroatomic/homoatomic, respectively. The 5d orbitals on Au, Hg, and Tl were not included in later calculations after they were found to yield only low-lying core-like bands, although proper relativistic calculations would involve these better.

Results and Discussion

Structure. These new ternary intermetallics crystallize in the orthorhombic space group *Imma* (No. 74) in a prototypical $CeCu_2$-type structure,[29] which is also known for the relevant $SrAl_2$,[30] $BaIn_2$,[31] $CaAu_2$, $SrAu_2$,[32] and KHg_2.[33] As shown in Figure 1, this structural topology in the (100) view can be described as a four-linked honeycomblike network (4^26^38)[34] of a $^3_\infty[Tr_2]^{2-}$ polyanion (Tr = Tl or In) with encapsulated Ba^{2+} cations, but with the majority Tl or In atoms now randomly replaced by 20(1)% Au in **1**, 18(2)% Au in **2**, or 46(1)% Hg in **3**. Each mixed M site has four like neighbors at three different distances (**I** (×2), **II**, **III**) that increase in that order (Figure 2a, Table 3) plus six Ba neighbors (Figure 2b). On the other hand, each Ba^{2+} counterion possesses 12 M neighbors (Figure 2a) at around 3.53−3.77 Å. The M substructure can be described in terms of rather flat six-membered rings with chair conformations that contain bonds **I** and **II** and are further fused along *a* and *c* to generate puckered 2D three-linked layers (6^3 nets) that lie around the (020) planes. Adjoining layers are further pillared alternately "up" and "down" at the zigzag chains along *a* by additional type **III** bonds to generate "zigzag ladders" of edge-sharing squares and the 4^26^38 network. Similar "zigzag ladders" are found in other solid-state frameworks, $BaTl_4$[16] ($SrIn_4$-type[7]), Ba_2AuTl_7,[11] $BaAuTl_3$[12] ($BaAl_4$-type[15]), and Sr_3In_5[8] (Ca_3Ga_5-type[35]), for example, in which different connectivities between neighboring "zigzag ladders" result in different sizes and shapes of channels. On the other hand, the present 3D polyanion network can also be viewed as a condensed version of similar layers in black phosphorus (*Cmca*),[36] puckered 2D layers of six-membered

(22) Earnshaw, A. *Introduction to Magnetochemistry*; Academic Press: London, 1968; p 4.
(23) Ren, J.; Liang, W.; Whangbo, M.-H. *CAESAR for Windows*; Prime-Color Software, Inc., North Carolina State University: Raleigh, NC, 1998.
(24) Hoffmann, R.-D.; Pöttgen, R. *Chem. Eur. J.* **2001**, *7*, 382.
(25) (a) Whitmire, K. H.; Ryan, R. R.; Wasserman, H. J.; Albright, T. A.; Kang, S. K. *J. Am. Chem. Soc.* **1986**, *108*, 6831. (b) Janiak, C.; Hoffmann, R. J. *J. Am. Chem. Soc.* **1990**, *112*, 5924.
(26) Hinze, J.; Jaffé, H. H. *J. Chem. Phys.* **1963**, *67*, 1501.
(27) Komiya, S.; Albright, T. A.; Hoffmann, R.; Kochi, J. K. *J. Am. Chem. Soc.* **1977**, *99*, 8840.
(28) Alvarez, S. *Table of Parameters for Extended Hückel Calculations, Part 1*; Barcelona, Spain, 1987.
(29) Larson, A. C.; Cromer, D. T. *Acta Crystallogr.* **1961**, *14*, 73.
(30) Iandelli, A. *J. Less-Common Met.* **1987**, *135*, 195.
(31) Wendorff, M.; Röhr, C. *Z. Anorg. Allg. Chem.* **2005**, *631*, 338.
(32) Zachwieja, U. *J. Alloys Compd.* **1996**, *235*, 12.
(33) Duwell, E. J.; Baenziger, N. C. *Acta Crystalogr.* **1955**, *8*, 705.
(34) Wells, A. F. *Three-dimensional Nets and Polyhedra*; Wiley: New York, 1977; p 134.
(35) Cordier, G.; Schäfer, H.; Stetler, M. *Z. Anorg. Allg. Chem.* **1986**, *539*, 33.
(36) Brown, A.; Rundquist, S. *Acta Crystallogr.* **1965**, *19*, 684.

Table 3. Important Bond Lengths (Å) in **1**, **2**, and **3**

	1	**2**	**3**
M	0.20 Au + 0.80 Tl	0.18 Au + 0.82 In	0.46 Hg + 0.54 In
M−M × 2 (bond **I**)[a]	2.9793(9)	2.953(1)	2.9699(8)
M−M (bond **II**)[a]	3.021(2)	2.972(2)	3.009(2)
M−M (bond **III**)[a]	3.303(2)	3.246(3)	3.294(2)
M-Ba × 4	3.544(1)	3.529(1)	3.546(1)
M-Ba × 4	3.755(1)	3.780(1)	3.7706(1)
M-Ba × 2	3.617(2)	3.593(2)	3.604(1)
M-Ba × 2	3.694(2)	3.681(2)	3.674(1)

[a] Defined in Figure 2.

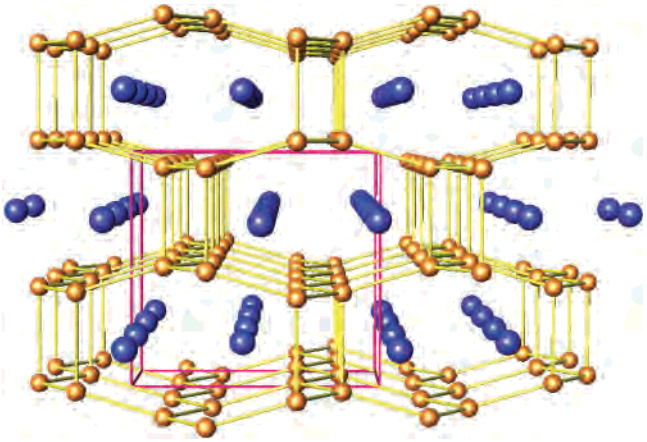

Figure 1. A [100] perspective view of the orthorhombic four-linked 4^26^38 network in $BaAu_{0.40(2)}Tl_{1.60(7)}$ (**1**), $BaAu_{0.36(4)}In_{1.64(4)}$ (**2**), and $BaHg_{0.92(2)}In_{1.08(2)}$ (**3**). The Ba and M (Tr + Au or Hg) atoms are blue and orange, respectively.

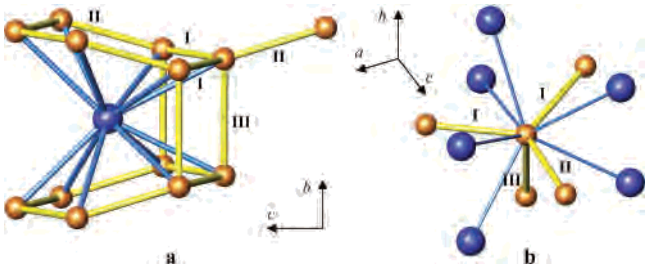

Figure 2. Local coordination environments of (a) the Ba atom (blue) and (b) the mixed M atoms (orange) in the three $CeCu_2$-type examples **1**, **2**, and **3**. The Ba and M atoms are blue and orange, respectively. Bonds **I** and **II** lie approximately parallel to the *ac* plane, and **III** lies along the *b* axis (Figure 1).

rings in chair conformations that have been further linked to each other via bonds between "up−down" members of neighboring layers.

The bond distances in all three compounds lie within reasonable ranges as estimated from standard metal−metal single bond distances. Powder patterns and unit cell parameters for a range of homogeneous $BaAu_xIn_{2-x}$ ($0 \le x \le 0.4$) variations of **2** are given in the Supporting Information, and the cell volume data are plotted in Figure 3. Compared with the cell volume of their parent $BaIn_2$ (378.2(4) Å^3), the volumes of the gold-substituted phases in the same structure type clearly contract with increasing *x*, 2.8% overall for ∼20% substitution in **2**. Likewise, the cell volume of $BaHg_{0.92(2)}In_{1.08(2)}$, and even of $BaAu_{0.40(2)}Tl_{1.60(7)}$ as well, are smaller than that for $BaIn_2$. Similarly, the M−M distances in both the six-membered rings and between these nets (**III**) in $BaAu_{0.40(2)}Tl_{1.60(7)}$ are shorter than those in the related

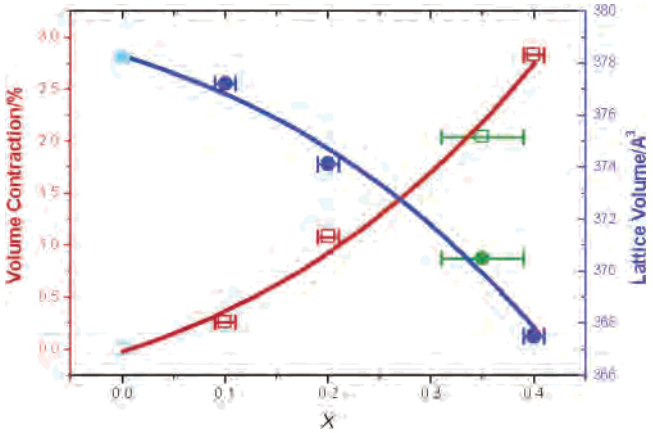

Figure 3. Volume dependencies of $BaAu_xIn_{2-x}$ (**2**) unit cells as a function of the Au concentration, *x*. Lattice volumes from powder refinements are blue, that for $x = 0$ (light blue) is from ref 31, and that from the single crystal study ($x = 0.36$) is green. Error bars in composition are $\pm 1\sigma$ values.

Table 4. Some Metal−Metal Distances (Å) in the Polyanion Nets of **1**, **2**, and **3** and in Related Compounds

compound	structure type	intralayer M−M (**I**, **II**)	interlayer M−M (**III**)
$BaTl_2$[a]	$CaIn_2$, $P6_3/mmc$	3.17	3.47
$BaAu_{0.40(2)}Tl_{1.60(7)}$ (**1**)	$CeCu_2$, *Imma*	2.98 × 2, 3.02	3.30
$BaIn_2$[b]	$CeCu_2$, *Imma*	3.02 × 2, 2.98	3.10
$BaAu_{0.36(4)}In_{1.64(4)}$ (**2**)	$CeCu_2$, *Imma*	2.95 × 2, 2.97	3.25
$BaHg_{0.92(2)}In_{1.08(2)}$ (**3**)	$CeCu_2$, *Imma*	2.97 × 2, 3.01	3.29

[a] Reference 20. [b] Reference 31.

hexagonal $BaTl_2$ ($CaIn_2$-type[20,37]) (Table 4), but larger than those in the rather different $BaAu_2$ (AlB_2-type[15]). The M−M distances in the six-membered rings in $BaAu_{0.36(4)}In_{1.64(4)}$ are somewhat shorter than those in the isostructural $BaIn_2$[31] On the other hand, the M−M interlayer distance is now clearly longer, by 0.15 Å at the limit, and this is reflected in an increasing *c* axis lengths as well. It is well known that relativistic effects[38] are ubiquitous for the more central 6th periodic elements, and gold is particularly famous for this.[39] Thus, these contractions of metal−metal distances distinctly reflect the relativistic size effect for gold, i.e., the contraction of the 6s orbital. The numbers of electrons in these systems also decrease on Au or Hg substitution, but later calculations show that the electrons removed are bonding, not antibonding, in character. Bond shrinkage in $BaHg_{0.92(2)}In_{1.08(2)}$ is not as large as with Au, consistent with the fact that relativistic effects with mercury are not as large.[38,39]

(37) Iandelli, A. *Z. Anorg. Allg. Chem.* **1964**, *330*, 221.
(38) Pyykkö, P. *Chem. Rev.* **1988**, *88*, 63.
(39) Pyykkö, P. *Angew. Chem., Int. Ed.* **2002**, *41*, 3573.

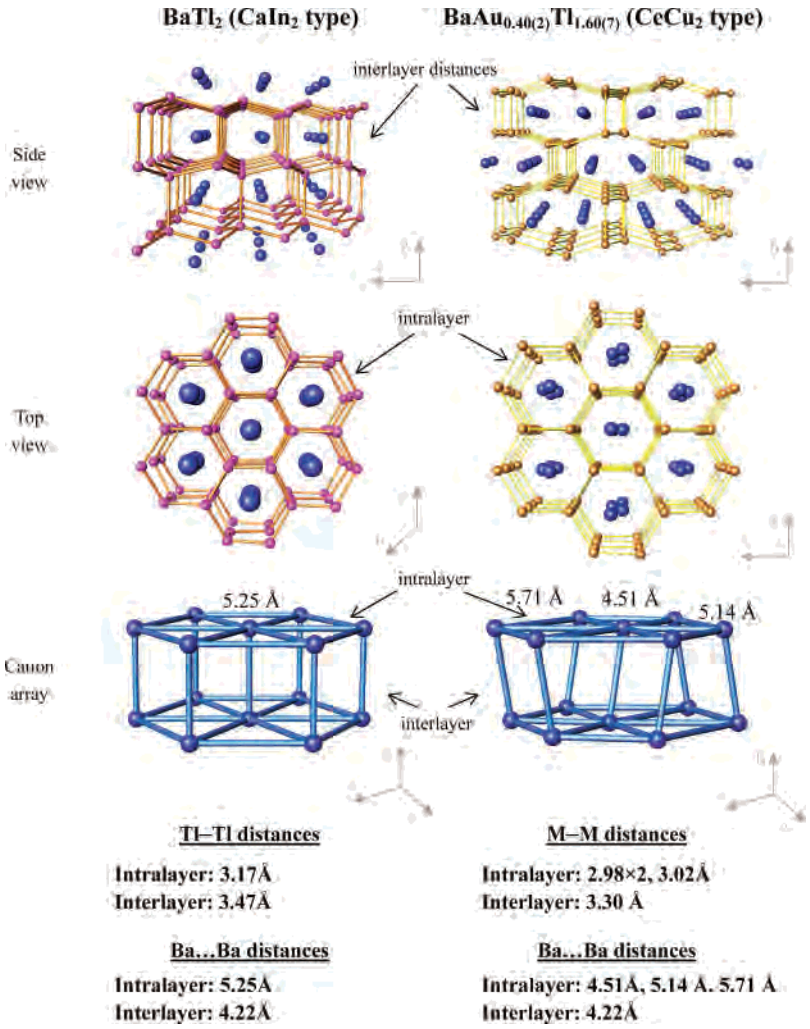

Figure 4. Side, top, and cation array views in a comparison of (left) the related $BaTl_2$ ($P6_3/mmc$) with (right) $BaAu_{0.40(2)}Tl_{1.60(7)}$ (*Imma*) (**1**) structural dispositions. The blue spheres represent Ba; red, Tl; orange, M (Au +Tl).

As with $BaAl_4$-type structures,[12,40,41] the hexagonal $CaIn_2$-type family of compounds may also exhibit matrix effects arising from symmetry and the relative atom sizes and bond lengths. An interesting question regarding compound **1** is the reason $BaAu_{0.40(2)}Tl_{1.60(7)}$ crystallizes with an orthorhombic $CeCu_2$-type structure rather than that of the parent hexagonal $BaTl_2$ ($CaIn_2$-type, $P6_3/mmc$). The two examples are contrasted in Figure 4 from several different aspects. In $BaTl_2$, the polyanionic network has appreciably longer Tl−Tl (M−M) bonds, 3.47 Å for the interlayer connections (between neighboring 6^3nets) and 3.17 Å within, affording a presumably good packing result for the encapsulated Ba^{2+} cations (Figure 4 (left), top and middle). These lie between puckered six-membered Tl rings at 3.49 (×6) and 3.91 (×6) Å distances with Ba···Ba separations of 5.25 Å parallel to the sheets and 4.22 Å between them (Figure 4 (left), bottom). However, judging from the observed product, insertion of 20% Au atoms into the polyanion network in the hexagonal phase would decrease the framework M−M bonds from 3.17 Å to an average of about 3.00 Å within the six-membered rings and from 3.47 to 3.30 Å between them. The Ba−M distances would in turn be decreased from 3.49 and 3.91 Å to ∼3.38 and ∼3.69 Å, respectively. (Both statements assume that Au substitution in the $BaTl_2$ structure would yield the same numerical results as observed in the orthorhombic product.) Generally, a tight packing is apparently present between network anions and the encapsulated cations in many examples of such polar intermetallic "salts", particularly those with +2 or +3 oxidation state cations. This is presumably what forces the observed transition to the lower-symmetry $CeCu_2$-type structure, a situation in which the cation retains 12 network neighbors, but these are spread over four larger Ba−M distances, particularly for the shorter contacts, 3.54−3.69 Å (Figure 2a, Table 3, Figure 4 (right)). (Alternatively, of course, the heteroatom packing could be left largely unchanged, leaving the network bonds in the hexagonal phase overly long.) Similar matrix effects are better known among the more frequently studied and higher-symmetry $BaAl_4$-type examples.[12,40,41] Although it is harder to judge the effects of changes in the cation lattice alone on formation of **1**, this results in an offset or slipped cation network with Ba···Ba separations that average 5.21 Å (4.51−5.71 Å) in baricentered six-membered rings within the sheets

(40) Häussermann, U.; Amerioun, S.; Eriksson, L.; Lee, C.-S.; Miller, G. J. *J. Am. Chem. Soc.* **2002**, *124*, 4371.
(41) Burdett, J. K.; Miller, G. J. *Chem. Mater.* **1990**, *2*, 12.

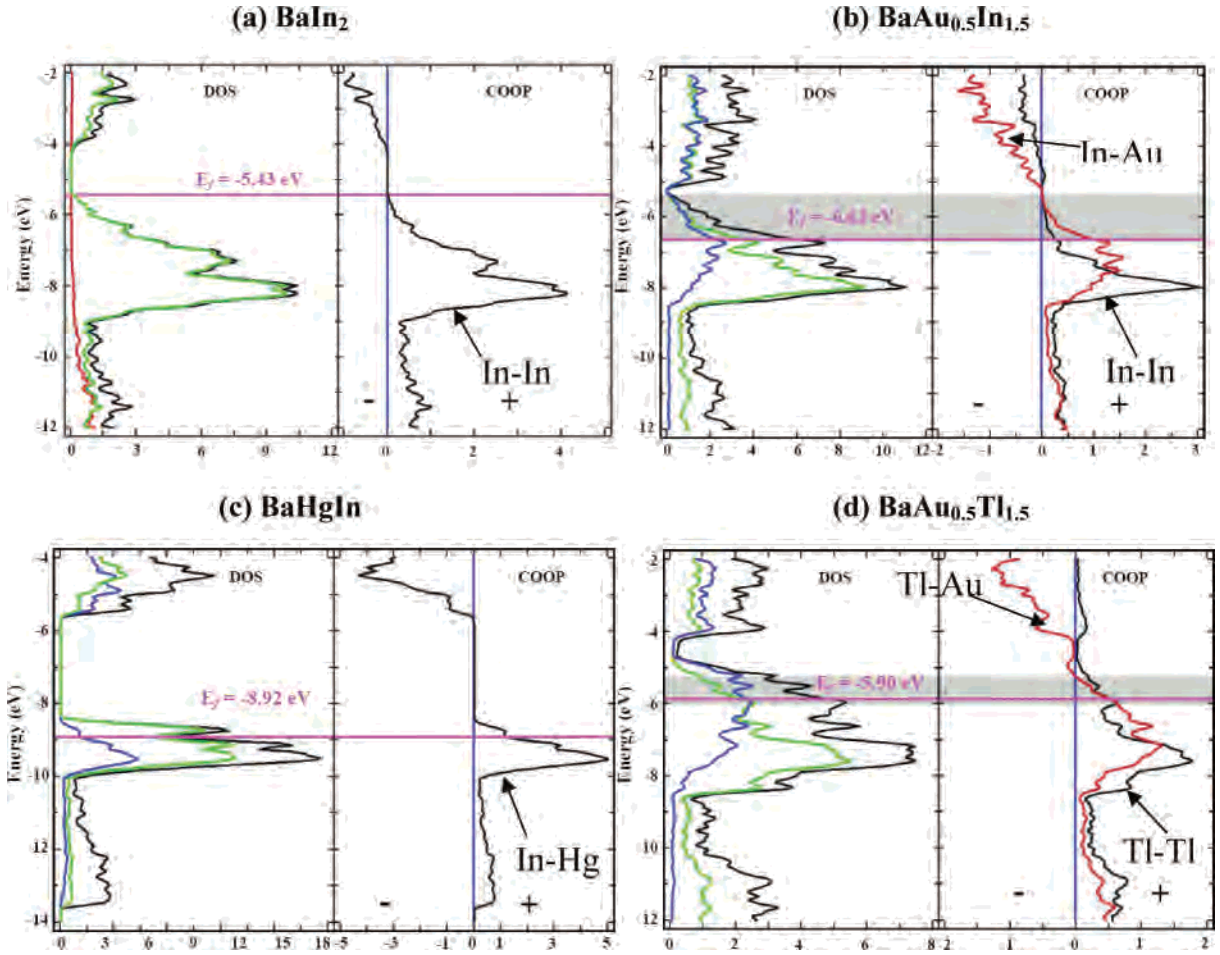

Figure 5. Densities-of-states (DOS) and the crystal orbital overlap population (COOP) results for $BaIn_2$ (a) and for the approximations $BaAu_{0.5}In_{1.5}$ for **2** (b), BaHgIn for **3** (c), and $BaAu_{0.5}Tl_{1.5}$ for **1** (d), all $CeCu_2$ type. The lines on the left refer to total DOS (black) and PDOS of In s state (red) and of In or Tl p (green) and M p orbitals (blue). COOP data are as labeled as to bond types. The gray bands in (b) and (d) represent the Fermi-level range (rigid band) for the observed variations in stoichiometry.

vs a single 5.25 Å in the centered rings in $BaTl_2$—Figure 4, bottom. The shorter interlayer Ba···Ba spacings remain at 4.22 Å in both. The differences do not seem very definitive. Similar but simpler matrix effects can be recognized in the structure changes for $CaIn_2$[37] vs $CaAu_2$[32] and $CaIn_2$ vs $BaIn_2$[31] in which the smaller Au in the former pair and the larger Ba in the latter lead to $CeCu_2$-type structures rather than hexagonal $CaIn_2$ version. The general nature of this particular transformation has been discussed before on geometrical and theoretical grounds, the important feature being that the lower-symmetry $CeCu_2$ version affords increased lattice flexibility, in particular, distortions that accompany the formation of two 90° angles around the formerly tetrahedral network sites allow larger cations to be accommodated.[42]

Chemical Bonding and Electronic Structures. Figure 5 illustrates the total and projected partial densities-of-states (DOS) and the crystal orbital overlap populations (COOP) for $BaIn_2$ and as approximated for **2**, **3**, and **1** (EHTB). (The data actually pertain to 25% Au and 50% Hg in ordered, lower-symmetry anion lattices—see Experimental Section.) The contributions to valence bands come mainly from p orbitals on M atoms, with only small contributions to DOS (<4%) from Ba 6s (not shown), in accord with the general ideas of the Zintl concept.[43] (The Ba contributions are probably underestimated, particularly the effects of its 5d orbitals, which appear more important in some ab initio treatments,[44] and the band gaps are probably exaggerated.) Bonding in $BaIn_2$ appears to be optimized, and the phase would be a semiconductor by this criterion. The valence bands in the ternary systems, largely p in character, narrow appreciably only for Hg, for which the valence orbitals lie at lower energies. Otherwise, the valence bands in the electron-poorer ternaries are generally incompletely filled, and the phases are presumably metallic, as was established experimentally for **1**. The accompanying COOP data for the ternary gold systems now describe separate Tr—Tr and Tr—Au components, but the pairs are quite similar. These results also indicate that the bond shortenings are intrinsic and not the result of emptying antibonding states. (The gray areas in Figure 5 represent the E_F ranges (according to a rigid band approximation) for the phase widths established for the two gold compounds, with E_F for the refined Au-richer structures that were used in the calculations marked by the red line.)

(42) Nuspl, G.; Polborn, K.; Evers, J.; Landrum, G. A.; Hoffmann, R. *Inorg. Chem.* **1996**, *35*, 6922.
(43) Schäfer, H.; Eisenmann, B.; Müller, W. *Angew. Chem., Int. Ed. Engl.* **1973**, *12*, 694.
(44) Mudring, A.-V.; Corbett, J. D. *J. Am. Chem. Soc.* **2004**, *126*, 5277.

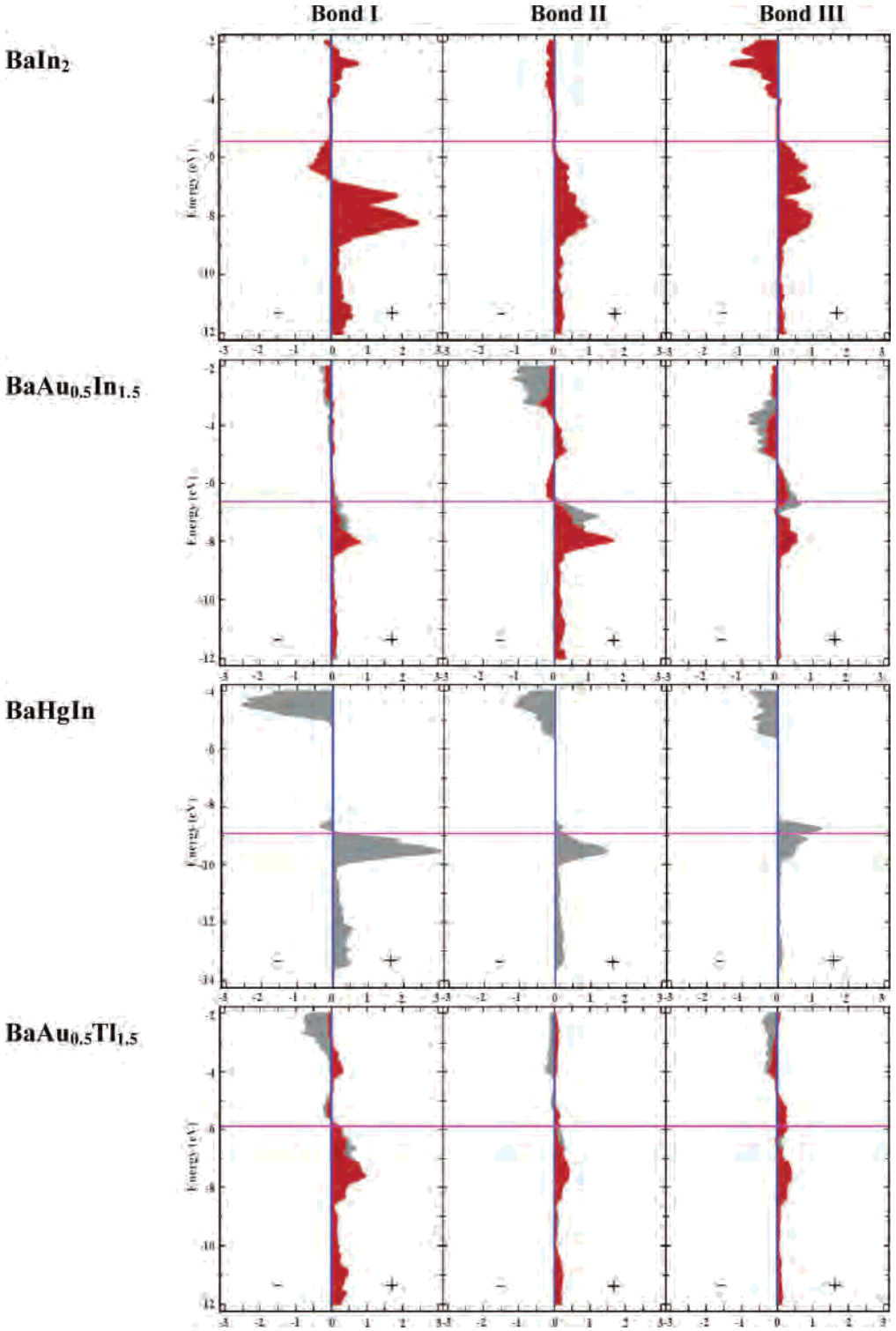

Figure 6. Crystal orbital overlap population (COOP) results for the three different M−M bonds types **I**, **II**, and **III** (see Figure 2) in $CeCu_2$-type frameworks of, top to bottom, $BaIn_2$ and the approximations $BaAu_{0.5}In_{1.5}$, BaHgIn, and $BaAu_{0.5}Tl_{1.5}$. Red areas represent homoatomic Tr−Tr bonds, and gray areas represent heteroatomic Tr−M bonds.

For $CeCu_2$-type structures, the stabilities of the framework are presumably also associated with their valence electronic counts. Earlier theoretical investigations indicated that the highest stability of the $CeCu_2$ structure should be at either 7[45] or 7.5 e^- per formula unit.[42] The refined results for the most oxidized (electron poorest) **1**, **2**, and **3** systems correspond to 7.2, 7.3, and 7.1 valence electrons per formula unit, respectively, close to the predictions. For **1** and **2**, the valence electron counts for the observed nonstoichiometry ranges correspond to about 7−7.8 and 7.2−8 e^- per formula unit, respectively, still close to general expectations.

In addition, the $CeCu_2$ structure contains three types of network bonds, two intralayer (**I** × 2, **II**) and one interlayer

(45) Lee, S. *J. Am. Chem. Soc.* **1991**, *113*, 101.

(**III**), which increase in length in that order, particularly for **III** (Figure 2, Table 4). (Note that the proportions of these three bond types in the structure heavily favor **I**; above.) Figure 6 presents detailed COOP schemes for each of the three characteristic bond types in $BaIn_2$, **2**, **3** and **1**, which in each case distinguish between the homoatomic (red) and heteroatomic (gray) bonds in the networks. The data in Figure 6 clearly show that states near the Fermi level for bond types **I**, **II**, and **III** all have substantially only positive COOP (bonding) contributions up to E_F in all three compounds. The smaller electron counts have also avoided the antibonding effects for bond **I** in $BaIn_2$, but other substantial changes are also seen. Distortions among the ternary structures appear to be effective in maintaining optimal bonding in most cases, a plausible corollary of the fact that we are always dealing with the thermodynamically most stable phases from high-temperature syntheses.

Acknowledgment. We are indebted to S. Budko for the magnetic susceptibility data.

Supporting Information Available: Additional crystallographic information for **1**, **2**, and **3**, unit cell parameters for a series of $CeCu_2$-type phases, powder patterns of the new phases that illustrate the existence of single phase regions of $BaAu_xTl_{2-x}$ and $BaAu_xIn_{2-x}$, and resistivity and magnetic susceptibility plots for **1**. This material is available free of charge via the Internet at http://pubs.acs.org.

IC051891K